Autonomous Flight in Unknown Indoor Environments

Autonomous Flight in Unknown Indoor Environments

Abraham Bachrach, Ruijie He and Nicholas Roy*
Massachusetts Institute of Technology, Cambridge, MA, USA

ABSTRACT

This paper presents our solution for enabling a quadrotor helicopter, equipped with a laser rangefinder sensor, to autonomously explore and map unstructured and unknown indoor environments. While these capabilities are already commodities on ground vehicles, air vehicles seeking the same performance face unique challenges. In this paper, we describe the difficulties in achieving fully autonomous helicopter flight, highlighting the differences between ground and helicopter robots that make it difficult to use algorithms that have been developed for ground robots. We then provide an overview of our solution to the key problems, including a multi-level sensing and control hierarchy, a high-speed laser scan-matching algorithm, an EKF for data fusion, a high-level SLAM implementation, and an exploration planner.[1] Finally, we show experimental results demonstrating the helicopter's ability to navigate accurately and autonomously in unknown environments.

1 INTRODUCTION

Micro Aerial Vehicles (MAVs) are increasingly being used in military and civilian domains, including surveillance operations, weather observation, and disaster relief coordination. Enabled by GPS and MEMS inertial sensors, MAVs that can fly in outdoor environments without human intervention have been developed [2, 3, 4, 5].

Unfortunately, most indoor environments and many parts of the urban canyon remain without access to external positioning systems such as GPS. Autonomous MAVs today are thus limited in their ability to fly through these areas. Traditionally, unmanned vehicles operating in GPS-denied environments can rely on dead reckoning for localization, but these measurements drift over time. Alternatively, simultaneous localization and mapping (SLAM) algorithms build a map of the environment around the vehicle while simultaneously using it to estimate the vehicle's position. Although there have been significant advances in developing accurate, drift-free SLAM algorithms for large-scale environments, these algorithms have focused almost exclusively on ground or underwater vehicles. In contrast, attempts to achieve the same results with MAVs have not been as successful due to a combination of limited payloads for sensing and computation, coupled with the fast, unstable dynamics of the air vehicles.

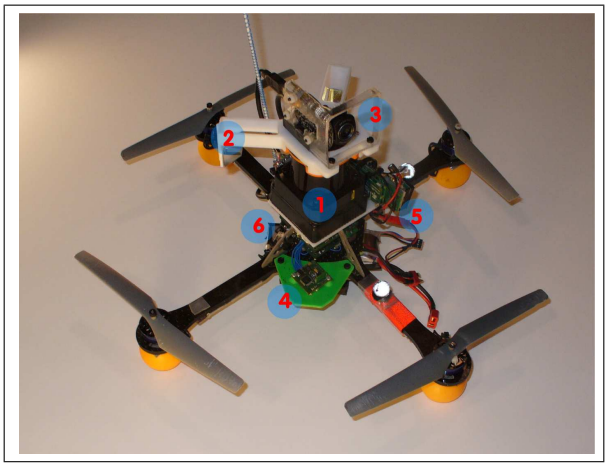

Figure 1: Our quadrotor helicopter. Sensing and computation components include a Hokuyo Laser Rangefinder (1), laser-deflecting mirrors for altitude (2), a monocular camera (3), an IMU (4), a Gumstix processor (5), and the helicopter's internal processor (6)

In this work, we present our quadrotor helicopter system, shown in Figure 1, that is capable of autonomous flight in unstructured indoor environments, such as the one shown in Figure 2. The system employs a multi-level sensor processing hierarchy designed to meet the requirements for controlling a helicopter. The key contribution of this paper is the development of a fully autonomous quadrotor that relies only on onboard sensors for stable control without requiring prior maps of the environment.

After discussing related work in Section 2, we begin in Section 3 by analyzing the key challenges MAVs face when attempting to perform SLAM. We then give an overview of the algorithms employed by our system. Finally, we demonstrate our helicopter navigating autonomously in 3 different unstructured indoor environments.

2 RELATED WORK

In recent years, autonomous flying robots has been an area of increasing research interest. Many capabilities have been developed for autonomous operations in outdoor environments, including high-speed flight through cluttered environments [3], helicopter acrobatics [4], autonomous landing

*Email addresses: {abachrac, ruijie, nickroy}@mit.edu

[1]The system described in this paper was originally presented for the 2009 European Micro Air Vehicle Conference [1]

Figure 2: Autonomous flight in unstructured indoor environments

and terrain mapping [5], coordinated tracking and planning of ground vehicles [2], etc. These systems typically take advantage of GPS measurements for state estimation, which are not available indoors.

While some authors [6, 7] have demonstrated indoor flight using GPS simulated from motion capture systems, we seek to develop flying robots that are able to operate autonomously while carrying all sensors used for localization, control and navigation onboard. Other authors [8, 9] use a small number of ultrasound sensors to perform altitude control and obstacle avoidance. Their helicopters are able to take-off, land and hover autonomously; however, they do not achieve goal-directed flight.

There have been numerous efforts to fly helicopters autonomously indoors using monocular camera sensors. [10] performed visual servoing over known Moire patterns to extract the full 6 degree-of-freedom state of the vehicle for control, while [11] detects lines in a hallway, and [12] tracked edges in office environments with known structure. While these authors have demonstrated autonomous flight in limited indoor environments, their approaches have been constrained to environments with specific features, and thus may not work as well for general navigation in GPS-denied environments. [13] extracted corner features that are fed into an EKF-based Vision-SLAM framework, building a low-resolution 3D map sufficient for localization and planning. However, an external motion capture system was used to simulate inertial sensor readings.

This paper builds on our previous work in [14], where we presented a planning algorithm for a laser-equipped quadrotor helicopter that is able to navigate autonomously indoors with a given map. Here, we extend the work by developing a system that is able to navigate, localize, build maps and explore autonomously *without* a prior map.

Recently, [15, 16] designed helicopter configurations that were similar to the one presented in [14]. [15] scan-matched successive laser scans to hover their quadrotor helicopter, while [16] used particle filter methods to globally localize their helicopter with a precomputed map that was generated by a ground-based robot. However, none of these papers present experimental results demonstrating the ability to stabilize all 6 *dof* of the helicopter autonomously using the onboard sensors.

3 MAV-Specific Challenges

In the ground robotics domain, combining wheel odometry with sensors such as laser rangefinders, sonars, or cameras in a probabilistic SLAM framework has proven very successful [17]. Many algorithms exist that accurately localize ground robots in large-scale environments. Unfortunately, the process of mounting equivalent sensors onto a helicopter and using existing SLAM algorithms does not result in the same success. The requirements and assumptions that can be made with flying robots are sufficiently different from those that can be made with ground robots that they must be managed differently.

3.1 Payload

MAVs have a maximum amount of vertical thrust that they can generate to remain airborne, which severely limits the amount of payload available for sensing and computation compared to similar sized ground vehicles. This weight limitation eliminates popular sensors such as SICK laser scanners, large-aperture cameras and high-fidelity IMUs. Instead, indoor air robots rely on lightweight Hokuyo laser scanners, micro cameras and/or lower-quality MEMS-based IMUs, all of which have limited ranges and fields-of-view and are noisier compared to their ground equivalents.

Unlike ground vehicles, air vehicles are unable to measure odometry directly; most SLAM algorithms need these measurements to initialize the estimates of the vehicle's motion between time steps. Although one can obtain relative position estimates by double-integrating acceleration measurements, lightweight MEMS-based IMUs are often subject to errors that introduce a bias that drifts very quickly. We must therefore obtain relative position estimates measurements by using either visual odometry [18] or laser scan-matching [19, 20] algorithms.

Finally, despite the advances within the community, SLAM algorithms continue to be computationally demanding even for powerful desktop computers, and are therefore not implementable on today's small embedded computer systems that can be mounted onboard indoor MAVs. The computation can be offloaded to a powerful groundstation by transmitting the sensor data wirelessly; however, communication bandwidth then becomes a bottleneck that constrains sensor options. Camera data must be compressed with lossy algorithms before it can be transmitted over WiFi links, which adds noise and delay to the measurements. This noise particularly affects feature detectors which look for high frequency information such as corners in an image. Additionally, while the delay can often be ignored for slow-moving, passively-stable ground robots, helicopters have fast and unstable dy-

namics, making control under large sensor delay conditions impossible.

3.2 Dynamics

The helicopter's fast dynamics result in a host of sensing, estimation, control and planning implications for the vehicle. Filtering techniques such as Kalman Filters are often used to obtain better estimates of the true vehicle state from noisy measurements. Smoothing the data generates a cleaner signal, but adds delay to the state estimates. While delays generally have insignificant effects on vehicles with slow dynamics, the effects are amplified by the MAV's fast dynamics.

In addition, as will be discussed in Section 4, the quadrotor is well-modeled as a simple 2^{nd}-order dynamic system with no damping. The underdamped nature of the dynamics model implies that simple proportional control techniques are insufficient to stabilize the vehicle, since any delay in the system will result in unstable oscillations. This effect has been observed experimentally. We must therefore add damping to the system through the feedback controller, which emphasizes the importance of obtaining accurate and timely state estimates for both position and velocity. Traditionally, most SLAM algorithms for ground robots completely ignore the velocity states.

Unlike ground vehicles, a MAV cannot simply stop and re-evaluate when its state estimates have large uncertainties. Instead, the vehicle is likely to be unable to estimate its velocity accurately, and may instead pick up speed or oscillate, degrading the sensor measurements further. Therefore, planning algorithms for air vehicles must not only be biased towards paths with smooth motions, but must also explicitly reason about uncertainty in path planning, as demonstrated in [14]; motivating our exploration strategy in Section 5.4.

3.3 3D effects

Finally, MAVs operate in a truly 3D environment since they can hover at different heights. The visible 2D slice of a 3D environment can change drastically with height and attitude, as obstacles suddenly appear or disappear. However, if we treat map changes resulting from changes in height and attitude as sensor errors, allowing the map to be updated to account for these changes, we will see that a 2D representation of the environment is surprisingly useful for MAV flight.

4 System Overview

We addressed the problem of autonomous indoor flight as primarily a software challenge, focusing on algorithms rather than exotic hardware. To that end, we used off-the-shelf hardware throughout the system. Our quadrotor helicopter, shown in Figure 1, is the AscTec Hummingbird from Ascending Technologies GmBH[2], and is able to carry roughly $250g$ of payload. We outfitted it with a Gumstix[3] microcomputer, which provides a WiFi link between the vehicle and a ground control station, and a lightweight Hokuyo[4] laser rangefinder for localization. The laser rangefinder provides a 270° field-of-view at $40Hz$, up to an effective range of $30m$. We deflect some of the laser beams downwards to estimate height above the ground plane.

The AscTec Hummingbird helicopter is equipped with attitude stabilization, using an onboard IMU and processor to stabilize the helicopter's pitch and roll [21]. This tames the nastiest portions of the quadrotor's extremely fast, nonlinear, and unstable dynamics [7], allowing us to focus on stabilizing the remaining degrees of freedom in position and heading. The onboard controller takes 4 inputs, $\mathbf{u} = [u_\phi, u_\psi, u_t, u_\theta]$, which denote the desired pitch and roll angles, overall thrust and yaw velocities respectively. The onboard controller allows the helicopter's dynamics to be approximated with simple 2^{nd}-order linear equations:

$$\begin{aligned} \ddot{x}^b &= k_\phi u_\phi + b_\phi & \ddot{z} &= k_t u_t + b_t \\ \ddot{y}^b &= k_\psi u_\psi + b_\psi & \dot{\theta} &= k_\theta u_\theta + b_\theta \end{aligned} \tag{1}$$

where $\ddot{x}^b$ and $\ddot{y}^b$ are the resultant accelerations in body coordinates, while k_* and b_* are model parameters that are functions of the underlying physical system. We learn these parameters by flying the helicopter inside a Vicon[5] motion capture system and fitting parameters to the data using a least-squares optimization method. We also experimented with a dynamics model that includes damping terms,

$$\ddot{s} = k_1 u + k_2 \dot{s} + b \tag{2}$$

However, when fitting this model to the data, we found that $k_2 \approx 0$, confirming pilot experience that the system is underdamped. Using the Matlab® linear quadratic regulator (LQR) toolbox, we then find feedback controller gains for the dynamics model in Equation 1.

To compute the high-precision, low-delay state estimates needed to stabilize the vehicle, we designed the 3-level sensing and control hierarchy, shown in Figure 3, distinguishing processes based on the real-time requirements of their respective outputs. This system was designed as a combination of asynchronous modules, building upon the CARMEN[6] robot navigation toolkit's software architecture. We describe the individual modules in the next section.

5 Enabling Technologies

5.1 Laser Scan-Matching Algorithm

As discussed in Section 3.1, we cannot directly measure the MAV's relative position. Instead, we align consecutive scans from the laser rangefinder to estimate the vehicle's motion using a standard technique from robotics known as scan-matching [22]. The goal of scan-matching is to find the most

[2]Ascending Technologies GmBH. `http://www.asctec.de`
[3]Gumstix Verdex. `http://www.gumstix.com`
[4]Hokuyo UTM-30LX Laser. `http://www.hokuyo-aut.jp`
[5]Vicon Motion Capture Systems. `http://www.vicon.com`
[6]CARMEN. `http://carmen.sourceforge.net`

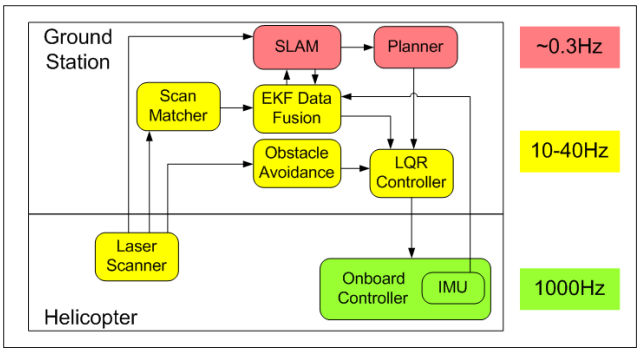

Figure 3: Schematic of our hierarchical sensing, control and planning system. At the base level, the onboard IMU and controller (green) create a tight feedback loop to stabilize the vehicle's pitch and roll. The yellow modules make up the real-time sensing and control loop that stabilize the vehicle's pose at the local level and avoids obstacles. Finally, the red modules provide the high-level mapping and planning functionalities.

likely alignment between pairs of laser scans, subject to the assumption that the same laser points are generated from the same physical object in the environment from time-step to time-step. Any deviation in the estimated range along the same bearing is assumed to be sensor noise. An additional constraint is that the alignment operator is a rigid body transformation on one of the scans, which corresponds to a rigid body transformation on the center of body of the vehicle. As a result, searching for the most likely alignment of laser scans corresponds to searching for the most likely motion of the vehicle between scans.

Scan-matching assumes that all range measurements are taken independently, which allows the likelihood of an alignment to be computed as the product of likelihoods for each individual point in the scan. There are a number of possible models of measurement likelihood. In our implementation, we follow Olson et al's model [20] of measurement likelihood of subsequent scans as a generative probabilistic model given by a Gaussian blur of a polygonal reduction of previous scans. That is, a representation of the previous scan is constructed as a set of piece-wise linear contours $\{C\}$, and the probability of a single lidar point (x, y) is approximated as proportional to the distance, d, to the nearest contour C_i, such that

$$P(x, y|C_i) \propto e^{(-d/\sigma)}$$

where σ is a variance parameter that accounts for the sensor's noise characteristics.

Given the likelihood model from a previous scan, scan-matching proceeds by searching for the rigid transform (x, y, θ) for a subsequent scan. Many scan-matching algorithms use gradient descent techniques to optimize these values. However, since the 3D pose likelihood space is often very complicated, even for fairly simple environments, gradient descent is subject to local optima. We instead use a very robust, if potentially computationally inefficient, exhaustive search over a grid of possible poses. While this exhaustive search might initially seem hopelessly inefficient, if implemented carefully, it can be performed fast enough to run in realtime. In our implementation, we use a grid spacing of $7.5mm$ in x, y, and $.15^\circ$ in θ. At this resolution, it takes approximately $5ms$ to search over the approximately $15,000$ candidate poses in the search grid to find the best pose for an incoming scan.

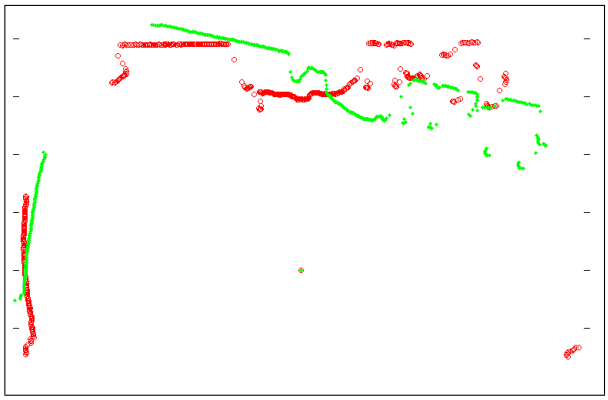

(a)

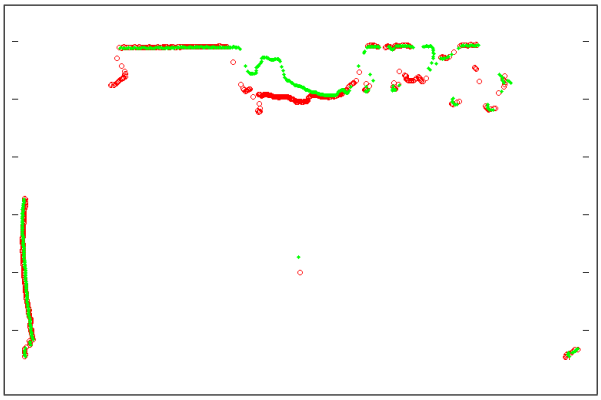

(b)

Figure 4: (a) Laser points from two consecutive scans. Notice that although the two scans cover much of the same area of the environment, a rotational error creates substantial misalignment. (b) The resulting scans after scan-matching. Although some parts of the scans still do not align due to occlusion, sensor error or 3D effects, the majority of the points overlap.

5.2 *EKF Data Fusion*

The scan matcher outputs the estimated vehicle position (x, y, θ), so to compute the full state estimate, including the velocities, we use an EKF to fuse the scan matcher estimates with the acceleration readings from the IMU. This has several advantages over directly using the position estimates from the

scan matcher and their derivatives to control the vehicle. Although the IMU readings drift significantly and are therefore not useful over extended time periods, they are useful over short time periods, allowing us to improve our estimate of the vehicle's velocities.

Our filter is a standard EKF, implemented using the open source KFilter library[7]. We use the filter to estimate the positions, velocities, and accelerations of the vehicle, along with the biases in the IMU. By flying the helicopter with the state estimation process running in a motion capture system, we obtain ground-truth values with which to compare our state estimates.

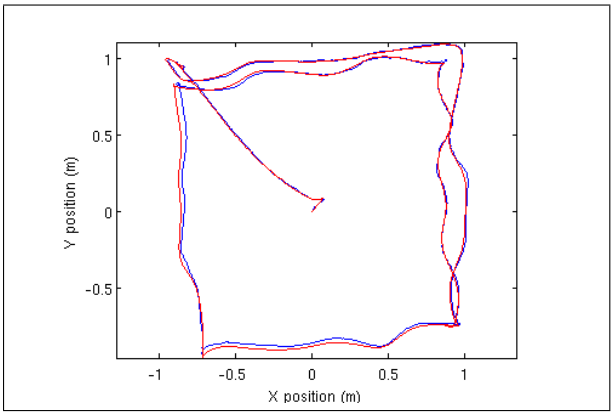

(a)

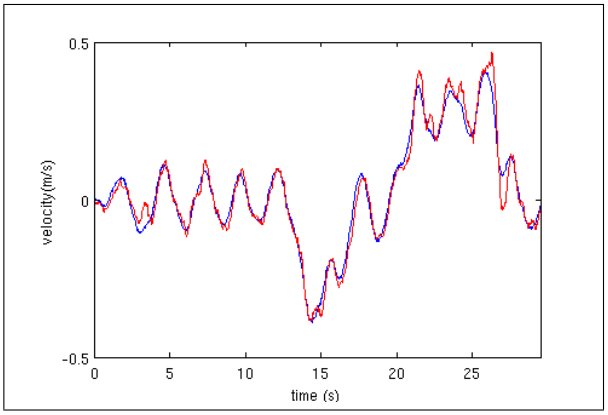

(b)

Figure 5: Comparison of the position (a) and velocity (b) estimated by the onboard sensors (red) with ground truth measurements (blue).

Figures 5(a) and 5(b) demonstrate the quality of our EKF state estimates. We compared the EKF state estimates with ground-truth state estimates recorded by the motion capture system, and found that the estimates originating from the laser range scans match the ground-truth values closely in both position and velocity. Throughout the 1min flight, the average distance between the two position estimates was less that $1.5cm$. The average velocity difference was $0.02m/s$, with a standard deviation of $0.025m/s$. The vehicle was not given any prior information of its environment (i.e., no map). However, since all the walls in the room were constantly within the laser's field-of-view in this experiment, the SLAM module was not needed to eliminate drift.

5.3 SLAM

We made use of the publicly available implementation of the GMapping [23] algorithm that is available in the OpenSlam repository[8], which performs SLAM in 2D. Despite the fact that the helicopter operates in the full 3D environment, the algorithm works surprisingly well and serves as a proof of concept for implementing SLAM on a MAV.

GMapping is an efficient Rao-Blackwellized particle filter which learns grid maps from laser range data. We chose it due to its outstanding accuracy, real-time performance, and its ability to handle changes to the 2D map that occur due to changing height and attitude, as discussed in Section 3.3. While the algorithm worked reasonably well out of the box, we made modifications that improved its performance when used in 3D environments on a MAV. The motion model for the particles in the GMapping algorithm was based on a standard motion model for ground robots with wheel odometry. However, since we use estimates computed by the laser scan matching module, we modified GMapping's motion model to propagate the particles using the uncertainties computed by the scan-matching module.

In addition to the motion model, we modified the map representation so that the map gets updated rapidly in response to changes in height. The algorithm computes the probability that each grid cell is occupied or free based on the number of times a laser beam reflects off, or passes through, the cell. If a particular cell has been hit many times, the algorithm places a very high confidence that the cell is occupied. However, if the helicopter changes heights, and the cell becomes part of free space, this confidence is no longer warranted. Unfortunately the laser must pass through the cell at least as many times as it was hit before the algorithm will be convinced that the cell is actually now free, resulting in a very slow adaptation of the map. Hence, we modified the map representation to cap the maximum confidence for each grid cell, allowing it to change from occluded to free (and vice-versa) more rapidly.

With these modifications, we are able to create large scale maps of the environment such as those shown in Section 6. The algorithm usually takes 1 to 2 seconds to process incoming laser scans, allowing it to be run online, but is not suitable to be directly incorporated into the real-time control loop. Instead, the GMapping algorithm periodically sends position corrections to the data fusion EKF. Since the position corrections are delayed significantly from when the measurement upon which they were based was published, we must account for this delay when we incorporate the correction.

[7] KFilter. `http://kalman.sourceforge.net`

[8] OpenSlam. `http://openslam.org`

This is done by retroactively modifying the appropriate position in the state history. All future state estimates are then recomputed from this corrected position, resulting in globally consistent state estimates. By incorporating the SLAM corrections after the fact, we allow the state estimates to be processed and published with low enough delay to control the MAV, while still incorporating the information from SLAM to ensure drift-free position estimates.

5.4 Planning and Exploration

In addition to computing globally consistent state estimates, the map generated by the SLAM algorithm is used to plan actions for the vehicle autonomously. Full autonomy requires a high-level planner that enables the MAV to explore environments without any human intervention. While exploration has been well-researched in ground robotics, differences between air and ground vehicles, as discussed in Section 3, require different considerations when deciding where to go next. In particular, the need to constantly provide control signals to the MAV means that while we seek to explore the environment, we must also ensure that the MAV always remains well-localized.

Our algorithm trades off the speed with which the helicopter completes coverage of the environment with safety, ensuring that there are known environmental features within the helicopter sensor's field-of-view as it uncovers unexplored environments. We use a modified definition of frontiers, first proposed in [24], to choose possible positions in free space where the MAV should fly to next such that it can make observations of previously unexplored regions in the environment. In [24], free cells that are adjacent to unknown cells are grouped into frontier regions as possible goals for the robot. We use a similar method to [24] to identify frontier regions, however, for each of these frontier regions, we seek to find a frontier pose that maximizes both the amount of unexplored space that is expected to be observed and the ability of the MAV to localize itself, which we define below.

The first step in our exploration algorithm is to identify candidate frontier regions. Frontier regions are areas in the map where there is a direct transition between free and unexplored cells. Since the walls in occupancy maps such as those generated by GMapping may have small gaps, the set of regions is then filtered to remove spurious frontiers. The algorithm must then identify the pose within these frontier regions that provides the best tradeoff between localization ability, and uncovered area. Searching over all poses in the frontier regions is too slow to allow the algorithm to run online, so frontier poses are sampled in each region. For each sample, two metrics are used to calculate a weight associated with each sample. First, the amount of unexplored space that the MAV will observe can be estimated by simulating the laser sensor data that the MAV is expected to obtain at the sampled pose, given the latest map. By extracting the number of grid cells within the laser's field-of-view that are currently unexplored and dividing by the maximum number of grid cells covered by a laser range scan, we get a normalized weight, $\mathcal{I}_{\mathcal{UR}}(x)$ in the range of $[0, 1]$ for the amount of unexplored information that the MAV is expected to observe.

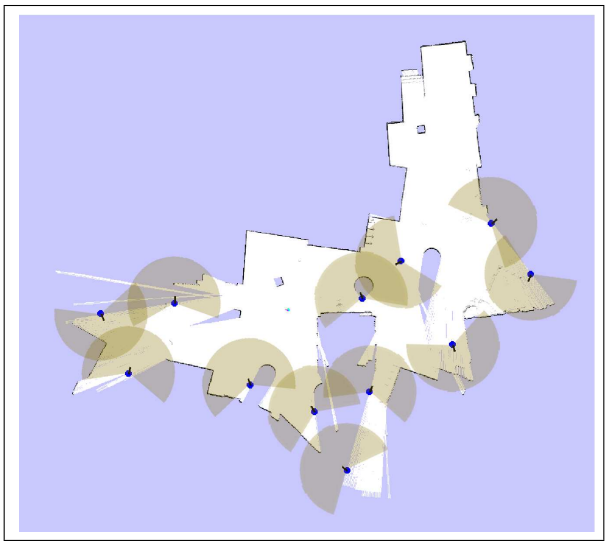

Figure 6: The blue pointers indicate frontiers that allow the MAV to explore and self-localize simultaneously. The laser's field-of-view at those frontiers is drawn in brown. Notice that at the edges of free space, the chosen frontiers position the vehicle such that the expected laser scan spans both unexplored regions for exploration and unique obstacles for localization.

Using this metric alone will result in frontier points that are at the extreme borders of the map facing the unexplored region, since such a pose will maximize the number of grid cells in the laser's field-of-view that are unexplored. Unfortunately, this pose provides no guarantees that the MAV will be able to localize itself, since the unknown environment may not contain enough structure for the relative position estimation algorithms to match against. In the extreme case, the MAV could be facing an open space where the nearest walls are beyond the maximum range of the laser scanner, giving the MAV no information with which to localize itself.

We therefore add an additional "Sensor Uncertainty" metric, first coined in [25]. Sensor uncertainty is used to quantify the MAV's ability to localize itself at different positions in the map. A sensor uncertainty field maps locations x in the map to expected information gain, $x \rightarrow \mathcal{I}_{\mathcal{SU}}(x)$, by calculating the difference in entropy of the prior and posterior distribution

$$\mathcal{I}_{\mathcal{SU}}(x) = H(p(x)) - H(p(x|z)) \tag{3}$$

where entropy is

$$H(p(x)) = -\int p(x) \log p(x) dx \tag{4}$$

Shown in [14], the measure of information gain for laser data is typically insensitive to the choice of prior. We therefore use

a constant prior $p(x) = \Sigma_0$ such that $H(p(x)) = C$, as well as Bayes' rule to compute $p(x|z) = p(z|x) \cdot p(x)$, such that

$$\mathcal{I}_{\mathcal{SU}}(x) = C - H(p(z|x))\Sigma_0 \quad (5)$$

We compute the entropy of $p(z|x)$ by deterministically extracting a set of sigma points [26], or samples along the main axes of the current covariance estimate, and observing how they are transformed when they are passed through the measurement function. For each sample, we simulate the sensor measurements and find the probability of observing the sensor measurement at each of the sigma points. The lower the probability of observation at the neighboring sigma points, the smaller the entropy of the posterior distribution, and therefore the greater the information gain. Locations with high information gain correspond to locations that generate sensor measurements that we expect to maximize the localization accuracy of the vehicle. After normalizing this with the prior entropy, $\mathcal{I}_{\mathcal{SU}}(x)$ is also a weight that lies in the range of $[0, 1]$.

Using these two weights, we are able to find frontiers that maximize both the exploration and localization capabilities of the MAV. In each frontier region, we sample a set of candidate poses, and accept as the goal point for that region, the sample that maximizes the weighted sum of the two information metrics, such that $\mathcal{I}(x) = \mathcal{I}_{\mathcal{UR}}(x) + \mathcal{I}_{\mathcal{SU}}(x)$. Figure 6 shows the frontier points generated accordingly, where points are chosen such that the expected laser scan will both uncover unexplored regions and observe known obstacles, enabling the MAV to simultaneously explore and localize.

To achieve autonomous exploration of an unknown environment, the planner uses the nearest frontier as its goal and computes a path using the dynamic programming-based path planner in the CARMEN robot navigation toolkit. The frontier extraction modules run fast enough that they are able to re-generate plans as the vehicle moves through the environment and as the map is updated.

6 Experiments and Results

We integrated the suite of technologies described above to perform autonomous navigation and exploration in unstructured and unknown indoor environments. In this section, we present results demonstrating that the system is capable of fully autonomous operation in a variety of indoor environments. To get a full picture of our system in action, we suggest that the reader also view the videos taken of these experiments available at: `http://groups.csail.mit.edu/rrg/videos.html`.

6.1 Autonomous navigation in open lobbies

We flew the vehicle across the first floor of MIT's Stata Center. The vehicle was not given a prior map of the environment, and flew autonomously using only sensors onboard the helicopter. In this experiment, the vehicle was guided by a human operator clicking high-level goals in the map that was being built in real-time, after which the planner planned the best path to the goal. The vehicle was able to localize itself and fly stably throughout the environment. Figure 7(a) shows the final map generated by the SLAM algorithm at the end of the experiment. During the 8min flight until the battery was exhausted, the vehicle flew a distance of $208.6m$.

6.2 Autonomous navigation in cluttered environments

While unstructured, the lack of clutter along the walls in the lobby environment allowed the 2D map assumption to hold fairly well. We next tested our system by flying through a cluttered lab space (Figure 2, insert of Figure 7(b)), operating close to the ground. At this height, chairs, desks, robots, plants, and other objects in the area caused the 2D cross-sectional scan obtained by the laser rangefinder to vary dramatically with changes in height, pitch, and roll. The resultant SLAM map of the environment is shown in Figure 7(b). The grey features littered within the otherwise free space denote the objects that clutter the environment and are occasionally sensed by the laser rangefinder. Despite the cluttered environment, our vehicle was able to localize itself and maintain a stable flight for 6min over a distance of $44.6m$, a feat that would not have been possible with a static map assumption.

6.3 Autonomous exploration in office hallways

Finally, to demonstrate fully autonomous operation of the vehicle, we closed the loop with our exploration algorithm, as discussed in Section 5.4. The helicopter was tasked to explore the hallway environment shown in the insert of Figure 7(c). Once the helicopter took off and began exploring, we had no human control over the helicopter's actions as it autonomously explored the unknown environment. The helicopter continuously searched for and generated paths to areas of new information. Figure 7(c) shows the map built from 7min of autonomous flight, after traveling a distance of $75.8m$.

7 Conclusion

In this work, we have developed a quadrotor helicopter that is capable of fully autonomous exploration in unstructured and unknown indoor environments without a prior map, relying solely on sensors onboard the vehicle. By reasoning about the key differences between autonomous ground and air vehicles, we have created a suite of algorithms that accounts for the unique characteristics of air vehicles for estimation, control and planning. Having developed a helicopter platform that has many of the capabilities of autonomous ground robots, we believe that there is great potential for future extensions of such platforms to operate in fully 3-dimensional environments.

Acknowledgments

Abraham Bachrach was supported by the ARO MAST CTA, Ruijie He was supported by the Republic of Singapore

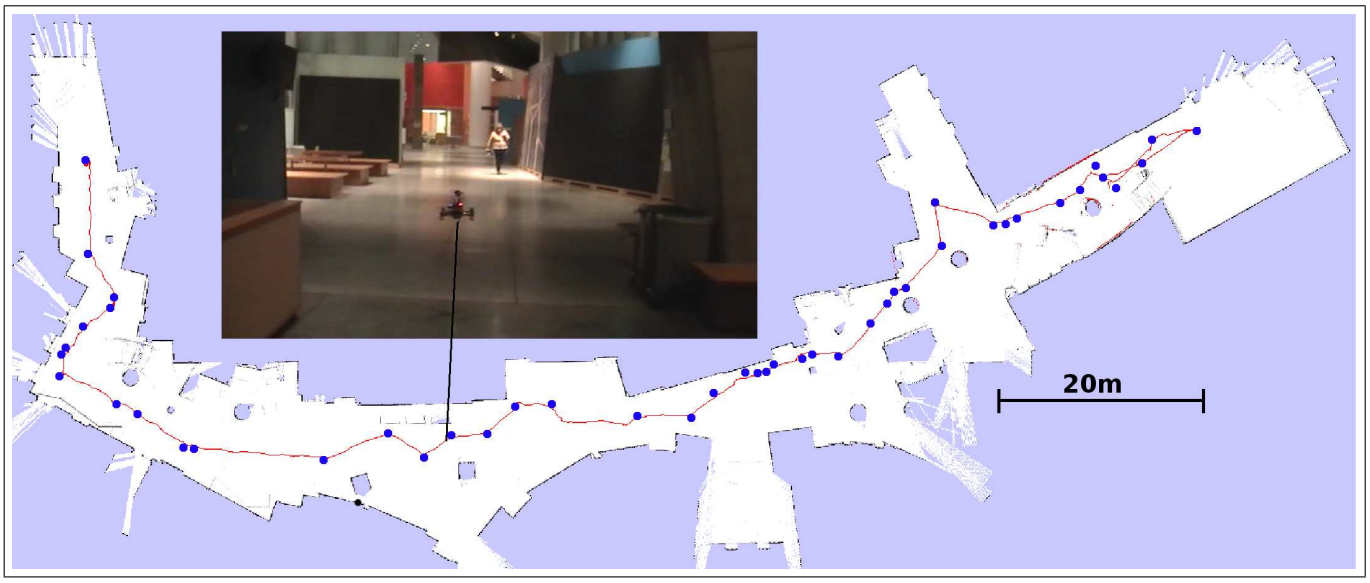

(a) Map of MIT Stata Center, 1st Floor.

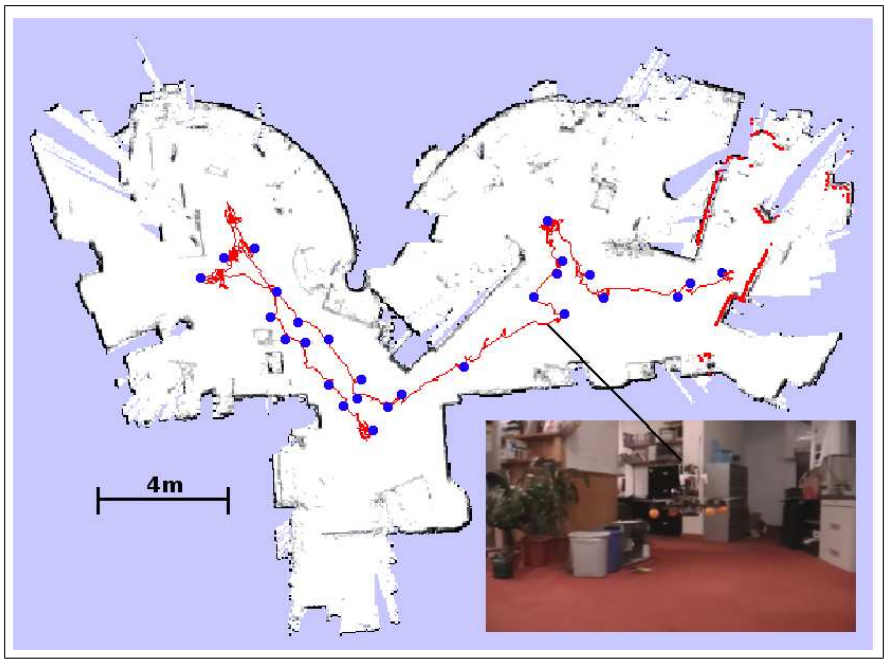

(b) Map of MIT Stata Center, 3rd Floor.

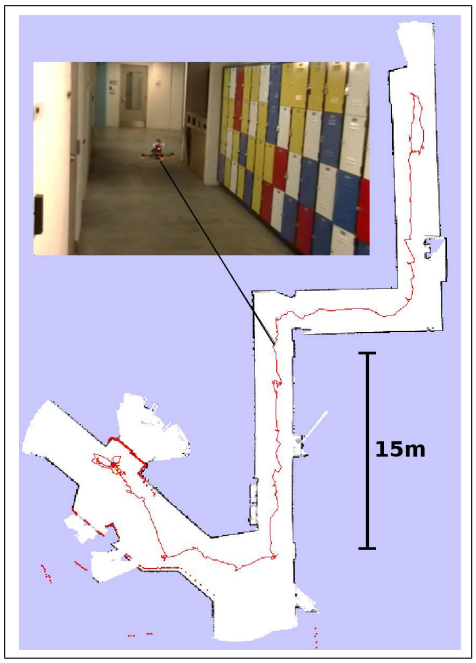

(c) Map of MIT Stata Center, basement.

Figure 7: (a) Map of the first floor of MIT's Stata center constructed by the vehicle during autonomous flight. (b) Map of a cluttered lab space with significant 3D structure. (c) Map of constrained office hallway generated under completely autonomous exploration. Blue circles indicate goal waypoints clicked by human operator. Red line indicates path traveled based on the vehicle's estimates.

Armed Forces, and Nicholas Roy was supported by NSF Division of Information and Intelligent Systems under grant # 0546467. The authors wish to thank the following people for their support in the project: Giorgio Grisetti, Cyrill Stachniss and Wolfram Burgard provided the GMapping software toolkit. Daniel Gurdan, Jan Stumpf and Markus Achtelik provided the quadrotor helicopter and the support of Ascending Technologies. Edwin Olson for providing us with a reference implementation of his scan-matcher. Samuel Prentice and Garrett Hemann assisted with the development of the hard-

ware.

REFERENCES

[1] A. Bachrach, R. He, and N. Roy. Autonomous flight in unstructed and unknown indoor environments. In *Proceedings of EMAV*, 2009.

[2] A. Bachrach, A. Garamifard, D. Gurdan, R. He, S. Prentice, J. Stumpf, and N. Roy. Co-ordinated tracking and planning using air and ground vehicles. In *Proc. ISER*, 2008.

[3] S. Scherer, S. Singh, L. Chamberlain, and S. Saripalli. Flying Fast and Low Among Obstacles. In *Proc. ICRA*, pages 2023–2029, 2007.

[4] A. Coates, P. Abbeel, and A.Y. Ng. Learning for control from multiple demonstrations. In *Proc. ICML*, pages 144–151. ACM, 2008.

[5] T. Templeton, D.H. Shim, C. Geyer, and S.S. Sastry. Autonomous Vision-based Landing and Terrain Mapping Using an MPC-controlled Unmanned Rotorcraft. In *Proc. ICRA*, pages 1349–1356, 2007.

[6] J.P. How, B. Bethke, A. Frank, D. Dale, and J. Vian. Real-time indoor autonomous vehicle test environment. *Control Systems Magazine, IEEE*, 28(2):51–64, 2008.

[7] G.M. Hoffmann, H. Huang, S.L. Waslander, and C.J. Tomlin. Quadrotor helicopter flight dynamics and control: Theory and experiment. In *Proc. of GNC*, Hilton Head, SC, August 2007.

[8] J.F. Roberts, T. Stirling, J.C. Zufferey, and D. Floreano. Quadrotor Using Minimal Sensing For Autonomous Indoor Flight. In *Proc. EMAV*, 2007.

[9] S. Bouabdallah, P. Murrieri, and R. Siegwart. Towards autonomous indoor micro vtol. Autonomous Robots, Vol. 18, No. 2, March 2005.

[10] G.P. Tournier, M. Valenti, J.P. How, and E. Feron. Estimation and control of a quadrotor vehicle using monocular vision and moirè patterns. In *Proc. of AIAA GNC, Keystone, Colorado*, 2006.

[11] N.G. Johnson. Vision-assisted control of a hovering air vehicle in an indoor setting. Master's thesis, BYU, 2008.

[12] C. Kemp. *Visual Control of a Miniature Quad-Rotor Helicopter*. PhD thesis, Churchill College, University of Cambridge, 2006.

[13] S. Ahrens, D. Levine, G. Andrews, and J.P. How. Vision-based guidance and control of a hovering vehicle in unknown, gps-denied environments. In *Robotics and Automation, 2009. ICRA '09. IEEE International Conference on*, pages 2643–2648, May 2009.

[14] R. He, S. Prentice, and N. Roy. Planning in information space for a quadrotor helicopter in a gps-denied environments. In *Proc. ICRA*, 2008.

[15] G. Angeletti, J.R. P. Valente, L. Iocchi, and D. Nardi. Autonomous indoor hovering with a quadrotor. In *Workshop Proc. SIMPAR*, pages 472–481, 2008.

[16] S. Grzonka, G. Grisetti, and W. Burgard. Towards a navigation system for autonomous indoor flying. In *Proc. ICRA*, 2009.

[17] S. Thrun, D. Fox, W. Burgard, and F. Dellaert. Robust monte carlo localization for mobile robots. *Artificial Intelligence*, 128:99–141, 2000.

[18] A. Howard. Real-time stereo visual odometry for autonomous ground vehicles. In *Proc. IROS*, 2008.

[19] Lingemann K., Nchter A., Hertzberg J., and Surmann H. High-speed laser localization for mobile robots. *Robotics and Autonomous Systems*, 51(4):275–296, June 2005.

[20] Edwin Olson. *Robust and Efficient Robotic Mapping*. PhD thesis, MIT, Cambridge, MA, USA, June 2008.

[21] D. Gurdan, J. Stumpf, M. Achtelik, K.M. Doth, G. Hirzinger, and D. Rus. Energy-efficient autonomous four-rotor flying robot controlled at 1 khz. In *Proc. ICRA*, 2007.

[22] F. Lu and E. Milios. Globally consistent range scan alignment for environment mapping. *Autonomous Robots*, 4:333–349, 1997.

[23] G. Grisetti, C. Stachniss, and W. Burgard. Improved techniques for grid mapping with rao-blackwellized particle filters. *IEEE Transactions on Robotics*, 23(1):34–46, 2007.

[24] B. Yamauchi. A frontier-based approach for autonomous exploration. In *Proc. CIRA*, 1997.

[25] H. Takeda and J.C. Latombe. Sensory uncertainty field for mobile robot navigation. *Proc. ICRA*, 1992.

[26] S.J. Julier, J.K. Uhlmann, and H.F. Durrant-Whyte. A new approach for filtering nonlinear systems. In *Proceedings of the American Control Conference*, volume 3, pages 1628–1632 vol.3, Jun 1995.